RSC Advances

ROYAL SOCIETY OF CHEMISTRY

www.rsc.org/advances

Single-Step Preparation of Recyclable Silver Nanoparticle Immobilized Porous Glass Filters for the Catalytic Reduction of Nitroarenes

*Hong-Ling Lin, Nga-Lai Sou, and Genin Gary Huang**

Department of Medicinal and Applied Chemistry, Kaohsiung Medical University,

Kaohsiung, 807, Taiwan

*To whom correspondence should be addressed.

E-mail: genin@kmu.edu.tw

Phone: +886-7-312-1101, ext. 2810

Fax: +886-7-312-5339

Abstract

In this study, a single-step preparation method for producing silver nanocatalysts was developed based on the silver-mirror reaction, and the prepared nanocatalysts were used in catalytically reducing nitroarenes. Sintered glass-filter discs were used as supports for the silver nanocatalysts not only to prevent the immobilized silver nanoparticles from aggregating but also to increase the loading capacity of the catalyst supports more effectively. Parameters that affect the morphologies of the prepared silver nanocatalysts, including the concentration of Ag^{+} in Tollen's reagent and porosity of the glass-filter supports are studied to obtain the appropriate morphologies for catalytically reducing 2-nitroaniline. Other factors that vary the efficiencies of the catalytic reduction, such as pH, temperature, the ability to reduce different nitroarenes, and the reusability of the silver catalysts were also studied to obtain a further understanding of the characteristics of the silver nanocatalysts prepared by conducting a silver-mirror reaction.

Introduction

Noble metals are generally considered to be stable and inert in bulk. However, the physical and chemical characteristics of nanosized noble materials are quite different from those in a macroscopic form, such as the quantum-tunneling effect,[1] surface-plasmon resonance,[2–4] and photothermal property.[5–7] Because of the unique and fascinating properties that can be observed after the nanonization of noble metals, noble metal nanomaterials have been applied extensively in various fields, including in sensing,[2–4,8–10] catalysis,[11-16] medical diagnosis,[7,17-19] surface-enhanced Raman scattering,[3,20-22] surface-enhanced fluorescence spectroscopy,[23-25] photothermal therapy,[17,26-28] antimicrobial agents,[29,30] and even for water purification.[31-33] In addition, the reduction of nitroarenes to aromatic amines is attracting increasing attention because of their industry importance and pharmaceutical necessity.[34-37] Various approaches have been investigated for reducing nitroarenes more efficiently and more rapidly, such as using noble-metal nanoparticles as catalysts,[12,16,38-41] combining graphene oxide (GO) or reduced graphene oxide (rGO) with noble nanoparticles as catalysts,[35,37,42,43] and using other hybrid nanocatalysts.[36,44,45] All of the aforementioned catalysis approaches are efficient and selective. However, the procedures for preparing nanocatalysts are rather complicated and time consuming. Besides, some of the reaction conditions are rather critical, e.g. refluxing. In this study, a simple but facile method was applied in preparing silver nanoparticles for use as catalysts for reducing nitroarenes. To prevent the reduced silver nanoparticles from aggregating, but also to increase the loading capacity of the catalyst supports, sintered glass-filter discs were used as the supports for the silver nanocatalysts. An additional advantage is that the recovering of the silver nanocatalysts from the reaction medium is easier comparing to load with other supports, such as silica gel. In fabricating silver nanocatalysts, silver-mirror reaction (Tollen's reagent) was engaged to simplify the

preparation procedure so that the nanocatalysts could be prepared in one-pot with a single step. Parameters that affect the morphologies of the prepared silver nanocatalysts and the efficiencies of the catalytic reduction, such as the concentration of Ag^+, porosity of the glass filters, pH, and temperatures, were studied systematically to acquire a broader understanding of the characteristics of silver nanocatalysts prepared by conducting a silver-mirror reaction.

Experimental Section

Materials

Sintered glass-filter discs with different pore sizes (14 to 40 μm with the average weight of 4.476 g, 40 to 100 μm with the average weight of 3.670 g, and 100 to 160 μm with the average weight of 3.762 g; diameter: 30 mm; thickness: 3.5 mm) were obtained from DURAN® (Mainz, Germany). Silver nitrate, o-nitroaniline (o-NA), m-nitroaniline (m-NA), and p-nitroaniline (p-NA) were purchased from Alfa Aesar. Sodium borohydride and dextrose were obtained from Acros Organics. Ammonium hydroxide and nitric acid were purchased from Fisher Scientific. Sodium hydroxide was obtained from Showa Chemical. All of the chemicals are reagent grade and were used as received without further purification. Deionized Milli-Q water (Simplicity™, Millipore) was used throughout the study.

Preparing Glass-Filter-Disc Supported Silver Nanocatalysts

All glass-filter discs were cut in half as the supports of the Ag nanocatalysts and treated with 3 h of 10% (v/v) ammonium-hydroxide aqueous solution followed by several times of rinsing with deionized water before loading with Ag nanocatalysts. Silver nanoparticles on glass-filter discs were reduced according to relevant literature.[46, 47] In brief, the glass-filter discs were immersed into 30 mL of Tollen's reagent, which consists of $AgNO_3$ ranging from 37.5 to 225 mM in concentration along with ammonia and dextrose, for 10 min. The concentration ratio of the

Ag^+:ammonia:dextrose was fixed at 1:6:10, and the deposition temperature was held in a 55 ^oC water bath. Field-emission scanning-electron microscopy (FE-SEM) was employed using a JSM-6330 TF microscope (Jeol) with an accelerating voltage of 10.0 kV to observe the morphologies of the prepared silver nanocatalysts. BET specific surface area of glass-filter discs were measured by an ASAP 2020 physisorption analyzer (Micromeritics Instrument Corporation).

Reduction of Nitroaniline Catalyzed by Silver Nanocatalysts

The catalytic efficiency of the porous glass filter-supported silver nanocatalysts was evaluated using the as-prepared silver nanocatalysts (half of a porous glass filter loaded with Ag nanocatalysts was used per reaction) in catalytically reducing o-NA. The prepared porous glass filter-supported silver nanocatalyst was gently placed in the 15 mL of aqueous solution consisting of 1 mM o-NA and 30 mM $NaBH_4$. UV/Vis spectra of the solution were recorded at chosen intervals; all UV/Vis spectra in this study were measured using a Thermo scientific Genesys 10S Bio UV/Visible spectrometer with a 1 nm resolution. A wavelength range from 250 to 550 nm was recorded, and the path length of the UV-Vis cell was 1 mm.

Results and Discussion

Effect of Ag^+ Concentration in Preparing Ag Nanocatalysts

Figure 1 depicts the SEM images of silver nanocatalysts prepared with different Ag^+ concentrations in Tollen's reagent (SEM images of smaller magnification are provided as Figure S1 in the electronic supplement information). As shown in the figure, the concentration of Ag^+ affected the morphologies of silver nanocatalysts considerably. When the concentration of Ag^+ was higher than 187.5 mM, the sizes of the reduced silver nanoparticles were larger than 100 nm, and an aggregation of silver nanoparticles was observed in which a continuous film was nearly formed when the Ag^+ concentration was 225 mM. In contrast, the sizes of formed silver nanoparticles

were approximately 100 nm, and no aggregation was found when the Ag^+ concentration was less than 150 mM. Moreover, the density of a silver nanoparticle depends on the Ag^+ concentration; the density approaches the maximum but the silver nanoparticles remain uncoagulated when the Ag^+ concentration is as high as 150 mM. Figure 2A shows the UV/Vis spectra of the reduction of o-NA catalyzed by silver nanocatalysts with increasing time when the as-prepared Ag nanoparticles immobilized glass filters are used as the catalysts for reducing o-NA. The absorbance peak located at 412 nm, which corresponded to the characteristic peak of o-NA,[48] decreased as the reaction proceeded. In addition, the absorbance peak located at 280 nm gradually shifted to 290 nm. These two spectra variations indicated that o-NA was reduced to 1,2-phenylenediamine.[12,40,42] The absorbance at 412 nm was recorded against the reaction time using the silver nanocatalysts prepared with different Ag^+ concentrations, and the results are plotted in Figure 3. For comparison, the results of a parallel experiment are also plotted in Figure 3. The reduction of o-NA can proceed only in the presence of silver nanocatalysts. In the absence of silver nanocatalysts, the reduction of o-NA is suspended even when the reaction is performed under refluxing for more than 8 h (the data between 30 min and 8 h are not shown). In addition, the reduction of o-NA was completed within 6 min when a Ag^+ concentration of 150 mM was used in Tollen's reagent, which has the best catalytic ability. It can also be deducted from Figure 1 and Figure 3 that the unaggregated silver nanoparticles exhibited superior efficiencies in reducing o-NA because the reduction of o-NA became slower as the concentration of the Ag^+ became higher than 187.5 mM in the preparation of the Ag nanocatalysts. The measured silver nanocatalysts mass loading prepared with different Ag^+ concentration are 2.29 % (w/w) for 225 mM Ag^+, 2.13 % (w/w) for 187.5 mM Ag^+, 2.11 % (w/w) for 150 mM Ag^+, 1.66 % (w/w) for 75 mM Ag^+, and 1.57 % (w/w) for 37.5 mM Ag^+, respectively. Although the silver

nanocatalysts mass loading increased as the Ag^+ concentration increased, the catalytic reduction efficiency didn't improve as well, which reveal that the size and the morphology of the prepared silver nanoparticle dominate the catalysis efficiency.

Effect of Glass-Filter-Disc Porosity

In catalytically reducing o-NA, the reaction was accelerated because the Ag nanocatalysts act as an electron relay between BH_4^- and o-NA.[39,49] The absorption of BH_4^- on the surface of the Ag nanocatalysts reduced the Fermi potential of the Ag nanocatalysts and resulted in an increase in the catalytic reduction rate. In addition, the catalytic reduction rate also depended on the number of Ag nanocatalysts.[49] To increase the number of Ag nanocatalysts on the glass-filter disc but also to increase the total surface area of the Ag nanocatalysts, three porosities of glass-filter discs were used as supports to prepare the silver nanocatalysts and were used in the catalytic reduction of o-NA. However, the larger the surface area the glass filters with a smaller pore size have, the larger the sizes and less dense the Ag nanoparticles observed on the glass-filter support, according to the SEM images (Figure S2 in the electronic supplement information). The smaller pore size may slow the rate of Tollen's reagent diffusing into the inner parts of the glass-filter supports. Figure 4 plots the absorbance of o-NA versus the reaction time by using Ag nanoparticles deposited on different porosities of glass-filter supports as catalysts. The figure indicates that the reduction of o-NA can be completed in 6 min by using both pore sizes of 40-100 μm and 100-160 μm sintered glass filters as the supports, whereas the reduction rate of the o-NA was decreased to 10 min by using a pore size of 40-100 μm glass-filter as the support. According to the SEM images, the prepared silver nanoparticle with the size of approximately 100 nm exhibits superior catalytic ability in reducing o-NA, which coincided with observations in the previous section. Meanwhile, the obtained BET surface area of the porous glass filter disc are 0.7854 m^2/g, 1.965 m^2/g, and 0.1265

m^2/g corresponded to the pore sizes of 100-160 μm, 40-100 μm, and 10-40 μm, respectively. The relative small BET surface area of the glass filter with the porosity of 10-40 μm may also limited the catalyst loading capacity and resulted in the longer reduction time.

Effect of Temperature and pH on the Catalysis Reaction

As described above, the main function of the silver nanocatalysts is to act as a relay between the nucleophile and electrophile. The catalyzed reduction rate is therefore affected by the electron abundance of the reaction system. To further confirm the role played by the Ag nanocatalysts in this study, the catalysis reaction was carried out under different pH conditions, and the absorbance at 412 nm was recorded against the reaction times under different pHs, with the results plotted in Figure 5. The pH played a key role in the catalysis reaction. When the pH was 10, the reduction of the 2-NA finished within 6 min while the reduction rate decreased dramatically when the pH was set at approximately 9, and only approximately 50 % of the 2-NA was reduced after 30 min of reduction. As the pH was tuned to be lower than 8, nearly no reduction of o-NA could be found. Therefore, the alkaline condition richened the electron densities on the Ag nanocatalyst surfaces, which promoted the reduction of the 2-NA.

In addition, the temperature of the catalytic reaction also influenced the rate of reduction because the reactants have a higher kinetic energy at higher temperatures and can more readily cross the activation state. Figure 6 depicts the relation between the absorbance at 412 nm and the reaction times under different reaction temperatures. As shown in Figure 6, the higher the temperature of the reaction system is, the faster the reduction of o-NA observed. In addition, the catalytic reduction of o-NA by using the Ag nanocatalysts prepared in this study could be accomplished quickly under rather mild conditions, which are more efficient and applicable in real utilities.

Capability of Ag Nanocatalysts in Accelerated Reduction of Other Nitroaniline

Isomers.

After examining the characteristics and the catalytic properties of the Ag nanocatalysts, the other two isomers of nitroaniline (m-NA and p-NA) were also catalytically reduced, according to the procedures established in the previous sections, to investigate the capability of the studied Ag nanocatalysts in promoting the reduction of other nitroarenes. Figure 2B and 2C plot the UV/Vis spectra of m-NA and p-NA reduced in the presence of Ag nanocatalysts with increasing times. The absorption maxima, which was located at 360 nm m-NA and 380 nm for p-NA,[16,36,44] decreased as the catalytic reduction proceeded. The relation between C_t/C_0 (C_0: absorbance at the initial time, C_t: absorbance after the specific reaction time) of three nitroanilines against the reaction time under the optimal condition was plotted as Figure 7. As the figure indicated, the reduction of o-NA and p-NA finished within 10 min where the reduction of m-NA finished with 20 min, which implies that the Ag nanocatalyst fabricated in this study is useful in catalytically reducing various nitroarenes. In order to compare our results to those of other studies, table 1 tabulated the catalytic activities of several supported noble nanoparticles systems. As can be observed in the table, the conversion efficiency of the porous glass filters supported silver nanocatalysts is as good as other reported noble nanoparticle catalysts. Furthermore, as reported in other works, the catalytic reduction of nitroarenes follows the pseudo-first-order reaction kinetics.[35,37] The relation between $\ln(C_0/C_t)$ of three nitroaniline isomers against the reaction time was also plot (Fig. S3) and the linear relations of all three nitroanilines were observed, which coincided with the behaviors of the pseudo-first-order reaction. The rate constant (k) at 50°C calculated from the slope to be 0.00940 s^{-1}, 0.00354 s^{-1}, and 0.00709 s^{-1} for the catalytic reduction of o-NA, m-NA, and p-NA by the silver nanocatalysts prepared in this study, respectively.

Recyclability of Ag Nanocatalysts.

Reusability of the silver nanocatalysts prepared in this study was evaluated by consecutively reusing the silver nanocatalyst for three times. According to Figure S4'; (a.), it's found that the about 70% of o-NA was converted to 1,2-phenylenediamine after 10 min of reaction in the second trial and only about 45% of o-NA was reduced after 10 min of reaction in the third time of usage where the reaction conditions were the same as the first run. The possible reason may be the adsorption of o-NA or 1,2-phenylenediamine on the surface of silver nanocatalysts, which decreased the electron transferability of the silver nanocatalysts. To further confirm this assumption, the silver nanocatalyst was soaked in a water solution with pH=3 for 20 min then immersed with neutral water in order the remove the adsorbed o-NA or 1,2-phenylenediamine before reusing the silver nanocatalyst. As can be seen in Figure S4(b.) in the electronic supplement information, more than 90% of o-NA can be reduced within 10 min after the second run, which coincided with the a assumption above. Therefore, the silver nanocatalysts fabricated in this study can be recycled after treated with acidic water solution, which extend the practical applicability of the silver nanocatalysts significantly.

Conclusion

In this study, silver nanoparticles were deposited on the surfaces of sintered glass filters by using a silver-mirror reaction and were used as the facile catalysts for reducing o-NA. Using the glass filters as the catalyst supports has the advantages of both keeping the morphologies of silver nanoparticles from aggregating and increasing the loading capacity of the silver nanocatalysts. An additional benefit of using the sintered glass-filter discs as supports is that the high cross-section prepares them for advanced application, such as for surface-enhanced Raman scattering. The results indicate that the morphologies of the deposited silver nanoparticles can be

varied by adjusting the concentration of Ag^+ in Tollen's reagent. In catalytically reducing o-NA, the reduction rate was affected by the pH of the system, temperature of the system, and porosity of the Ag nanocatalyst support. In addition, the prepared Ag nanocatalyst was effective in catalytically reducing other nitroarenes and can be recycled after treated with acidic water solution (pH=3). Finally, the proposed Ag nanocatalyst demonstrates the advantages of facile preparation, relatively mild catalytic conditions, and high catalytic ability, thus making it appropriate for use in advanced applications, which are currently undergoing further study.

Acknowledgement

We acknowledge the financial support of the Taiwan Ministry of Science and Technology under grant NSC102-2113-M-037-014-MY2, and NSYSU-KMU Joint Research Project NSYSUKMU 2013–P017.

References

(1) L. Mao, Z. Li, B. Wu and H. Xu, Appl. Phys. Lett., 2009, **94**, 243102.

(2) H. Ditlbacher, A. Hohenau, D. Wagner, U. Kreibig, M. Rogers, F. Hofer, F. Aussenegg and J. Krenn, Phys. Rev. Lett., 2005, **95**, 257403.

(3) K. A. Willets and R. P. Van Duyne, Annu. Rev. Phys. Chem., 2007, 58 267-297.

(4) J. Homola, Chem. Rev., 2008, **108**, 462-493.

(5) S. Link, and M. A. El-Sayed, Int. Rev. Phys. Chem., 2000, **19**, 409-453.

(6) X. Huang, I. H. El-Sayed, W. Qian and M. A. El-Sayed, J. Am. Chem. Soc., 2006, **128**, 2115-2120.

(7) P. K. Jain, X. Huang, I. H. El-Sayed and M. A. El-Sayed, Acc. Chem. Res., 2008, **41**, 1578-1586.

(8) K. M. Mayer and J. H. Hafner, Chem. Rev., 2011, **111**, 3828-3857.

(9) S. K. Ghosh and T. Pal, Chem. Rev., 2007, **107**, 4797-4862.

(10) S. Sumriddetchkajorn and K. Chaitavon, Appl. Opt., 2006, **45**, 172-177.

(11) M. Stratakis and H. Garcia, Chem. Rev., 2012, **112**, 4469-4506.

(12) B. Çelen, D. Ekiz, E. Pişkin and G. Demirel, J. Mol. Catal. A: Chem., 2011, **350**, 97-102.

(13) K. D. Bhatte, P. J. Tambade, K. P. Dhake and B. M. Bhanage, Catal. Commun., 2010, **11**, 1233-1237.

(14) W. Yan, R. Wang, Z. Xu, J. Xu, L. Lin, Z. Shen and Y. Zhou, J. Mol. Catal. A: Chem., 2006, **255**, 81-85.

(15) M.-C. Daniel and D. Astruc, Chem. Rev., 2003, **104**, 293-346.

(16) N. Pradhan, A. Pal and T. Pal, Colloids Surf., A, 2002, **196**, 247-257.

(17) X. Wang, C. Wang, L. Cheng, S.-T. Lee and Z. Liu, J. Am. Chem. Soc., 2012, **134**, 7414-7422.

(18) A. Ito, M. Shinkai, H. Honda and T. Kobayashi, J. Biosci. Bioeng., 2005, **100**, 1-11.

(19) S. P. Mulvaney and C. D. Keating, Anal. Chem., 2000, **72**, 145R-157R.

(20) J. Kneipp, B. Wittig, H. Bohr and K. Kneipp, Theor. Chem. Acc., 2009, **125**, 319-327.

(21) J. R. Lombardi and R. L. Birke, Acc. Chem. Res., 2009, **42**, 734-742.

(22) J. P. Camden, J. A. Dieringer, J. Zhao and R. P. V. Duyne, Acc. Chem. Res., 2008, **41**, 1653-1661.

(23) Y. Jiang, H.-Y. Wang, H. Wang, B.-R. Gao, Y.-W. Hao, Y. Jin, Q. –D. Chen and H.-B. Sun, J. Phys. Chem. C, 2011, **115**, 12636-12642.

(24) L. Touahir, A. T. A. Jenkins, R. Boukherroub, A. C. Gouget-Laemmel, J.-N. L. Chazalviel, J. Peretti, F. O. Ozanam and S. Szunerits, J. Phys. Chem. C, 2010, **114**, 22582-22589.

(25) M. K. Hossain, G. G. Huang, T. Kaneko and Y. Ozaki, Phys. Chem. Chem. Phys., 2009, **11**, 7484-7490.
(26) A. M. Gobin, M. H. Lee, N. J. Halas, W. D. James, R. A. Drezek and J. L. West, Nano Lett., 2007, **7**, 1929-1934.
(27) J. Nam, N. Won, H. Jin, H. Chung and S. Kim, J. Am. Chem. Soc., 2009, **131**, 13639-13645.
(28) S. Fazal, A. Jayasree, S. Sasidharan, M. Koyakutty, S. V. Nair and D. Menon, ACS Appl. Mater. Inter., 2014, **6**, 8080-8089.
(29) I. Sondi and B. Salopek-Sondi, J. Colloid Interface Sci., 2004, **275**, 177-182.
(30) J. Kim, E. Kuk, K. Yu, J. Kim, S. Park, H. Lee, S. Kim, Y. Park, Y. Park, C.-Y. Hwang, Y. Kim, Y. Lee, D. Jeong and M. Cho, Nanomedicine, 2007, **3**, 95-101.
(31) M. S. Bootharaju, G. K. Deepesh, T. Udayabhaskararao and T. Pradeep, J. Mater. Chem. A, 2013, **1**, 611-620.
(32) M. S. Bootharaju and T. Pradeep, Langmuir, 2012, **28**, 2671-2679.
(33) T. Pradeep and Anshup, Thin Solid Films, 2009, **517**, 6441-6478.
(34) P. K. Surolia, R. J. Tayade and R. V. Jasra, Ind. Eng. Chem. Res., 2010, **49**, 8908-8919.
(35) M.-Q. Yang, X. Pan, N. Zhang and Y.-J. Xu, CrystEngComm, 2013, **15**, 6819-6828.
(36) W. Wu, S. Liang, Y. Chen, L. Shen, H. Zheng and L. Wu, Catal. Commun., 2012, **17**, 39-42.
(37) Y. Choi, H. S. Bae, E. Seo, S. Jang, K. H. Park and B.-S. Kim, J. Mater. Chem., 2011, **21**, 15431-15436.
(38) T. Huang, F. Meng and L. Qi, J. Phys. Chem. C, 2009, **113**, 13636-13642.
(39] A. R. Kiasat, R. Mirzajani, F. Ataeian and M. Fallah-Mehrjardi, Chin. Chem. Lett., 2010, **21**, 1015-1019.
(40) L. Shi, Q. Yu, Y. Mao, H. Huang, H. Huang, Z. Ye and X. Peng, J. Mater. Chem., 2012, **22**, 21117-21124.
(41) J. Davarpanah and A. R. Kiasat, Catal. Commun., 2013, **41**, 6-11
(42) J. Huang, L. Zhang, B. Chen, N. Ji, F. Chen, Y. Zhang and Z. Zhang, Nanoscale, 2010, **2**, 2733-2738.
(43) R. Nie, J. Wang, L. Wang, Y. Qin, P. Chen and Z. Hou, Carbon, 2012, **50**, 586-596.
(44) F. Guo, Y. Ni, Y. Ma, N. Xiang and C. Liu, New J. Chem., 2014, **38**, 5324-5330.
(45) P. S. Rathore, R. Patidar, T. Shripathi and S. Thakore, Catal. Sci. Tech., 2015, **5**, 286-295.
(46) R.-L. J. Chang and J. Yang, Analyst, 2011, **136**, 2988-2995.
(47) M.-L. Cheng and J. Yang, Appl. Spectrosc., 2008, **62**, 1384-1394.

(48) X. Le, Z. Dong, W. Zhang, X. Li and J. Ma, J. Mol. Catal. A: Chem, 2014, **395**, 58-65.

(49) Z.-J. Jiang, C.-Y. Liu and L.-W. Sun, J. Phys. Chem. B, 2005, **109**, 1730-1735.

(50) Q. Zhou, G. Qian, Y. Li, G. Zhao, Y. Chao and J. Zheng, Thin Solid Films, 2008, **516**, 953-956.

(51) J. N. Solanki and Z. V. P. Murthy, Ind. Eng. Chem. Res., 2011, **50**, 7338-7344.

Figure Captions

Figure 1. SEM images of silver nanoparticles reduced on the sintered glass filter with a Ag^+ concentration of (a) 225 mM, (b) 187.5 mM, (c) 150 mM, (d) 75 mM, and (e) 37.5 mM. The concentration ratio of the Ag^+:ammonia:dextrose was fixed at 1:6:10, and the deposition was held in a 55 ^oC water bath for 10 min. The porosity of the glass filter was 40⁻100 μm, and the magnification of the images were all 50000x.

Figure 2. UV/Vis spectra of 1 mM (a) o-NA, (b) m-NA, and (c) p-NA reduced by 30 mM $NaBH_4$ at 50 ^oC in the presence of glass-filter supported silver nanoparticles with increasing times where the pH was 10. The Ag nanoparticles immobilized glass-filter fabrication condition was the same as described in Figure 1(c).

Figure 3. The absorbance of 1 mM o-NA (412 nm) versus the catalytic reduction time in the presence of 30 mM $NaBH_4$ and glass-filter supported silver nanoparticles prepared with (■) 37.5 mM, (●) 75 mM, (▲) 150 mM, (◆) 187.5 mM, and (▼) 225 mM Ag^+. The concentration ratio of the Ag^+:ammonia:dextrose in Tollen's reagent was fixed at 1:6:10. The deposition was held in a 55 ^oC water bath for 10 min, and the porosity of the glass filter was 40⁻100 μm. The catalytic reductions proceeded at 50 ^oC; and the pH was 10, whereas the parallel experiment (★) in the absence of silver nanocatalysts was refluxed.

Figure 4. The absorption time profile of 1 mM o-NA reduced by 30 mM $NaBH_4$ in the presence of glass-filter supported nanoparticles with (■) 100-160 μm, (●) 40-100 μm, and (▲) 16-40 μm of porosity. The Ag^+ concentration in Tollen's reagent was 150 mM, and the concentration ratio of the Ag^+:ammonia:dextrose in Tollen's reagent was fixed at 1:6:10. The deposition was held in a 55 ^oC water bath for 10 min, whereas the catalytic reductions proceeded at 50 ^oC and

a pH of 10.

Figure 5. The absorption time profile of 1 mM o-NA reduced by 30 mM $NaBH_4$ in the presence of glass-filter supported nanoparticles under different pH conditions where (■) pH=10, (●) pH=9, (▲) pH=8, (▼) pH=7, and (★) pH=6. The catalytic reductions proceeded at 50 ^oC, and the silver nanoparticles immobilized glass-filter fabrication condition was the same as described in Figure 1(c).

Figure 6. The absorption time profile of 1 mM o-NA reduced by 30 mM $NaBH_4$ in the presence of glass-filter supported nanoparticles at different temperatures where (■) 50 ^oC, (●) 44 ^oC, (▲) 38 ^oC, (▼) 25 ^oC, and (★) 0 ^oC. The pH of the solution was 10, and the silver nanoparticles immobilized glass-filter fabrication condition was the same as described in Figure 1(c).

Figure 7. The relation between C_t/C_0 (C_0: absorbance at the initial time, C_t: absorbance after the specific reaction time) of three nitroanilines (■: o-NA, ●: m-NA, and ▲: p-NA) against the reaction time reduced by 30 mM $NaBH_4$ in the presence of glass-filter supported nanoparticles at 50 ^oC. The pH of the solution was 10, and the silver nanoparticles immobilized glass-filter fabrication condition was the same as described in Figure 1(c).

Fig. 1

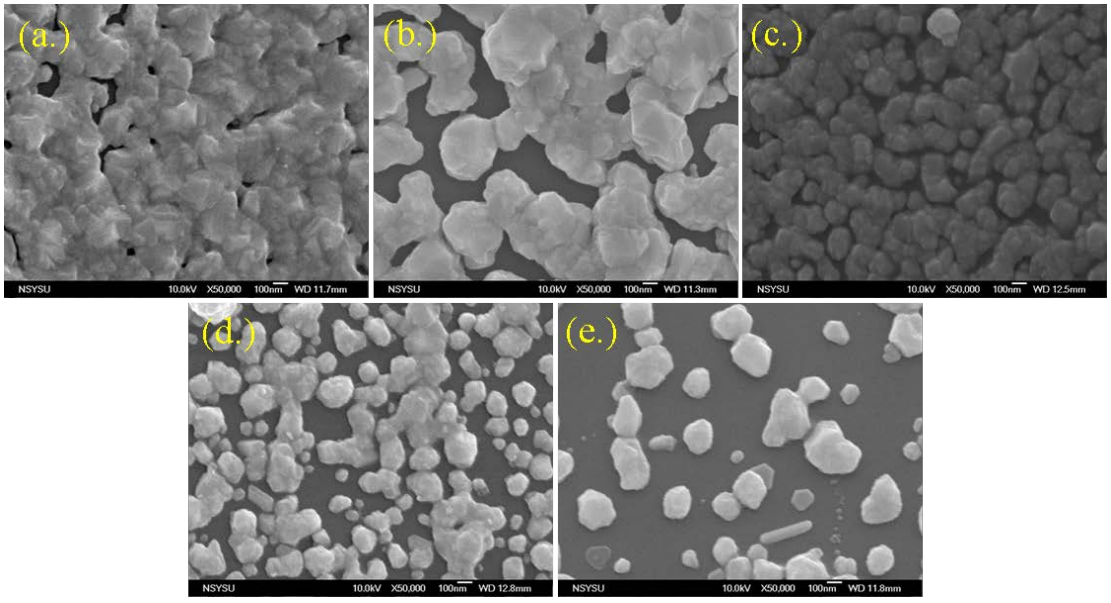

Fig. 2

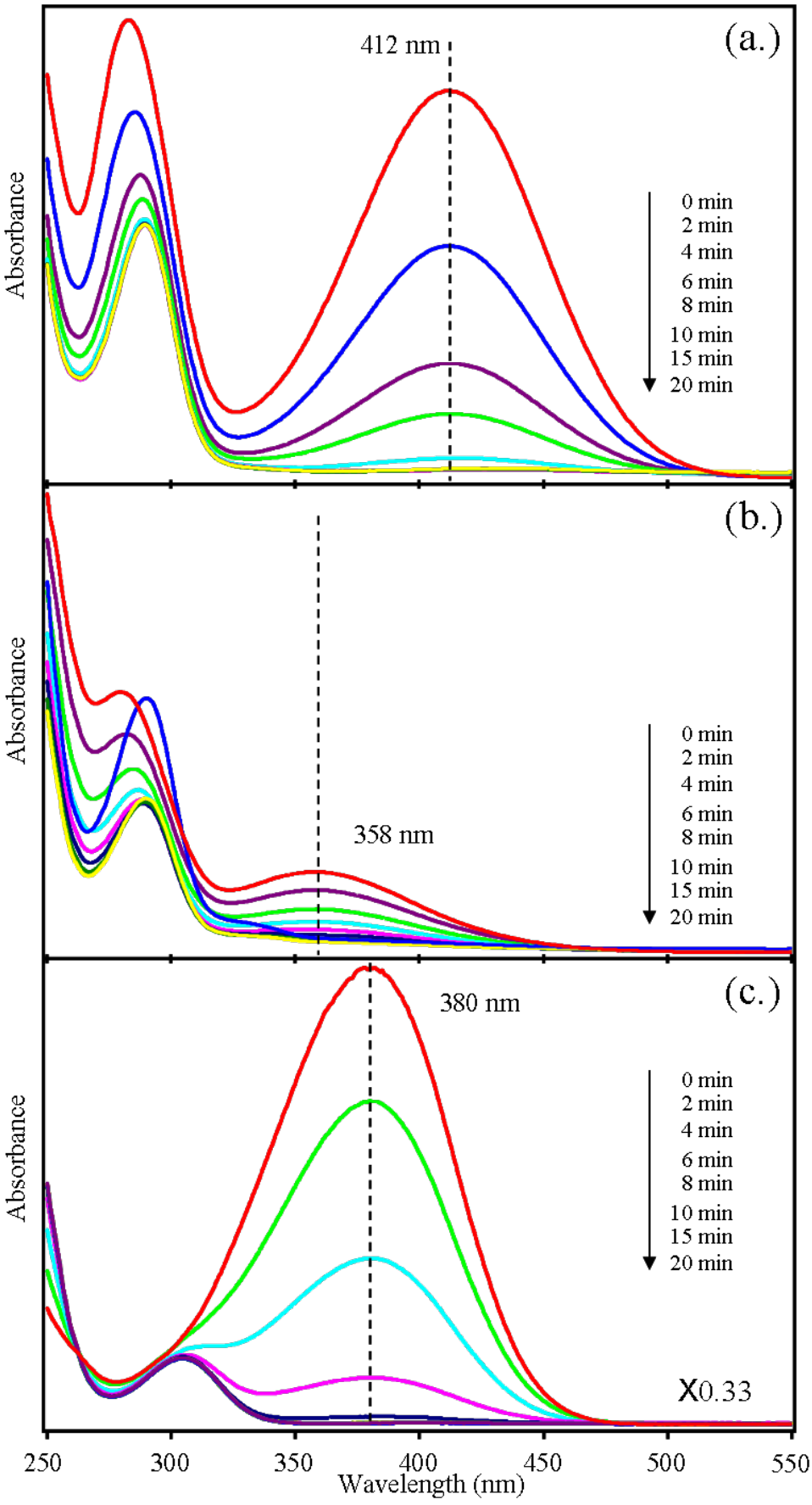

Fig. 3

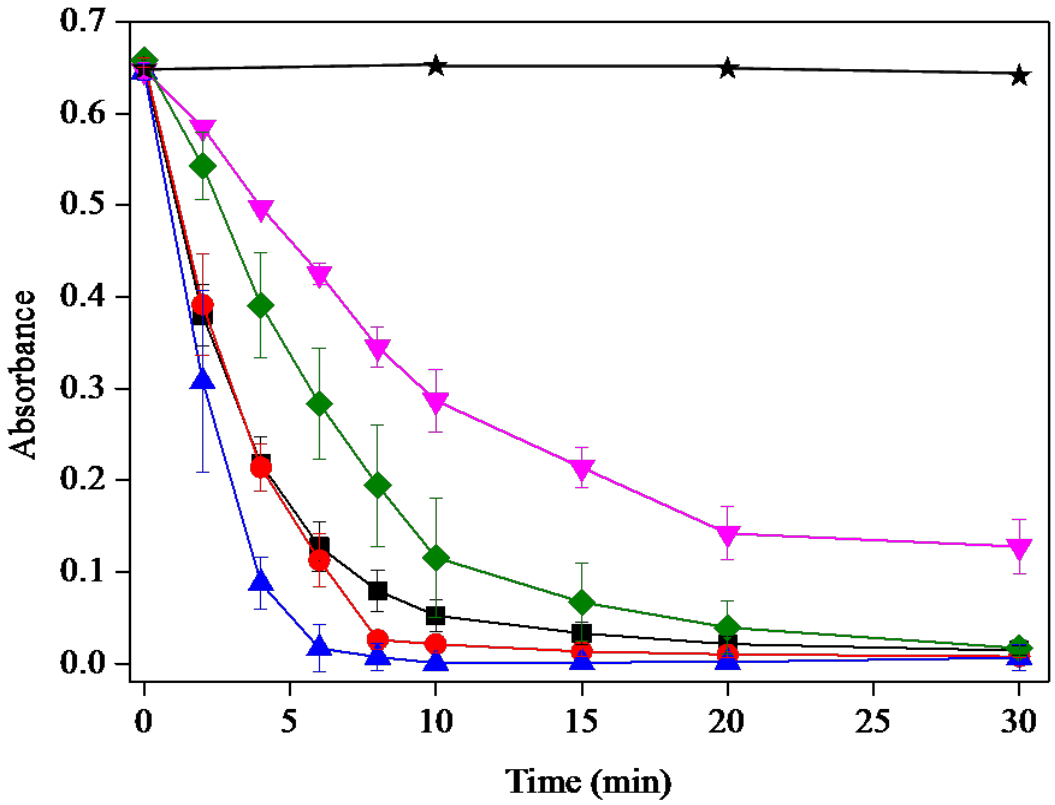

Fig. 4

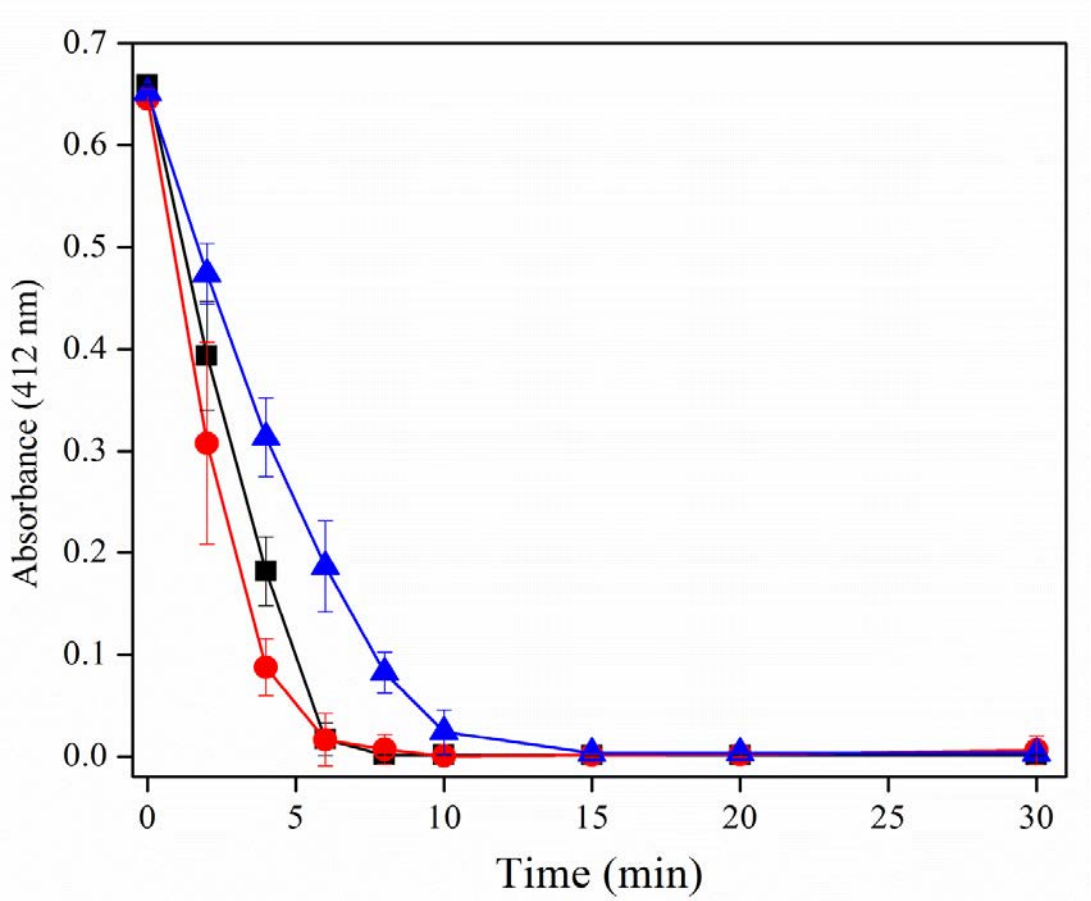

Fig. 5

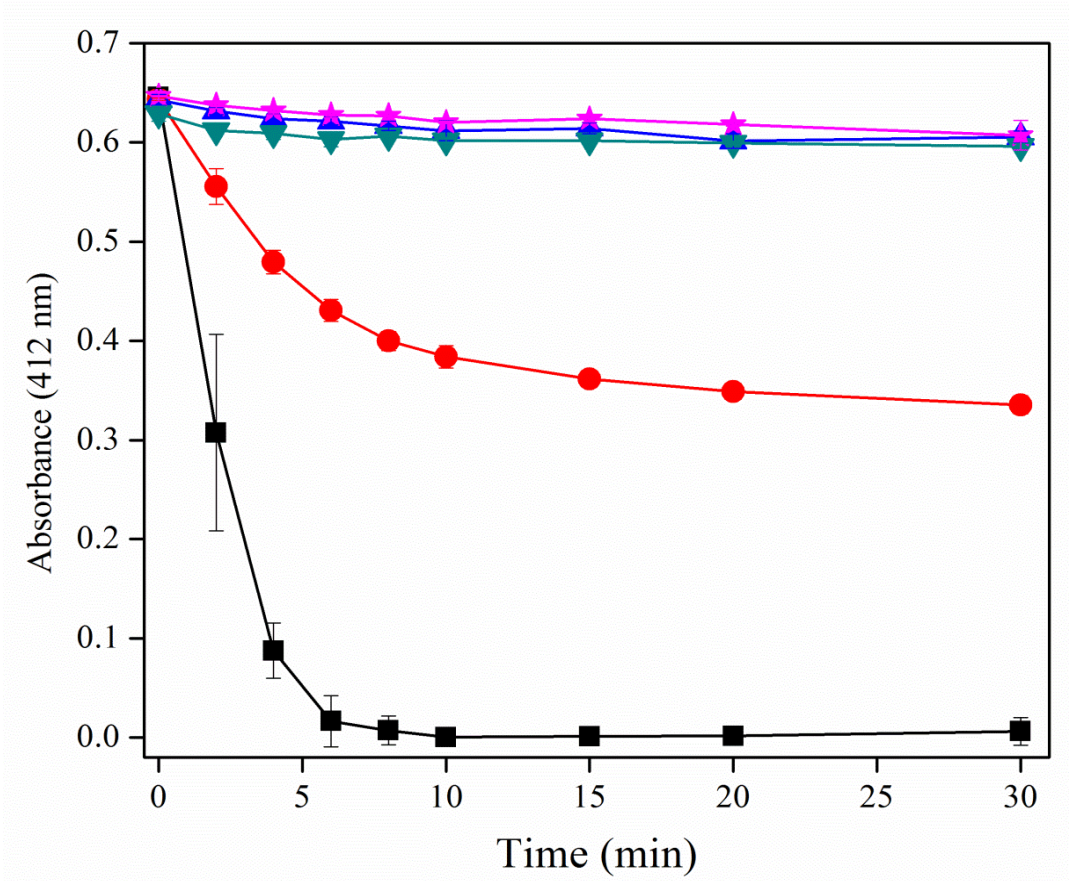

Fig. 6

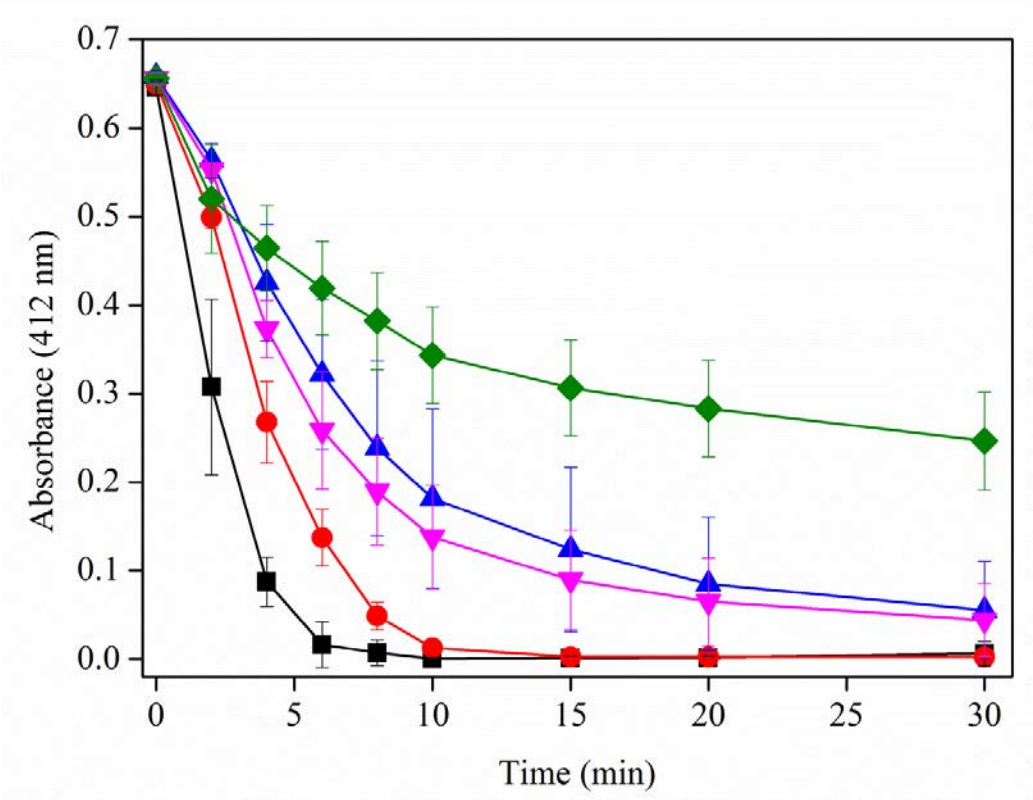

Fig. 7

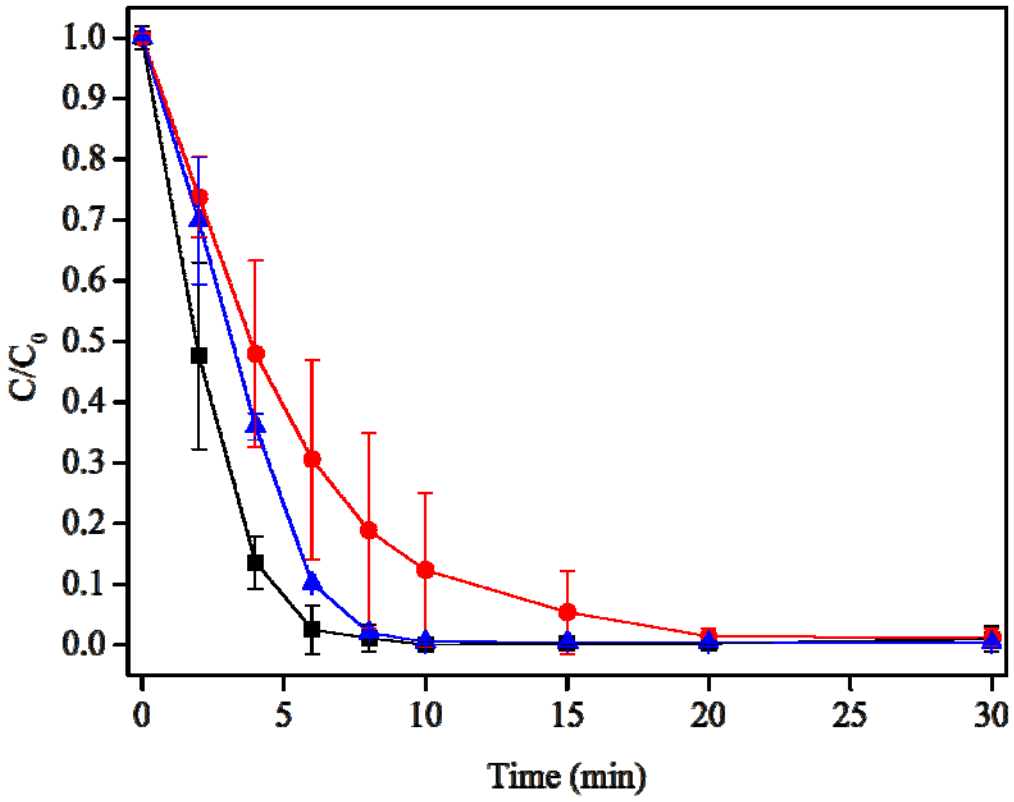

Table 1

Catalysts	Nitroarenes (final concentration)	Temperature	Conversion time	Ref.
AgNPs[a]/polydopamine/anodic aluminum oxide	o-NA (1.33 mM)	R.T.[b]	20 min	12
AgNPs/rice husk-SiO_2-aminopropylsilane	p-NA (1.00 mM)	100°C	75 min	41
AgNPs/partially reduced graphene oxide	p-NA (0.10 mM)	R.T.	4 min	35
AuNPs[c]/reduced graphene oxide nanosheets	o-NA (0.66 mM)	R.T.	14 min	37
	p-NA (0.66 mM)	R.T.	40 min	37
AuNPs/gelatin mesoporous composite thin films	o-NA (0.43 mM)	R.T.	10.5 min	40
AgNPs/Poly(vinylpyrrolidone) modified glass	p-NA (0.20 mM)	-[d]	27 min	50
AgNPs/Al_2O_3	p-NA (4.30 mM)	R.T.	26 min	51
This study	o-NA (1.00 mM)	50°C	6 min	
	p-NA (1.00 mM)	50°C	10 min	

a. silver nanoparticles; b. room temperature; c. gold nanoparticles; d. not mentioned.